BILINGUAL PUBLISHING CO.
Pioneer of Global Academics Since 1984

Journal of Mechanical Engineering Research
http://ojs.bilpublishing.com/index.php/jmer

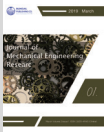

ARTICLE

Dynamic Analysis and Active Control of a Dielectric Elastomer Balloon Covered by a Protective Passive Layer

Zichen Deng[1,2*] Siqi An, Qingjun Li[1,2]

1.School of Mechanics, Civil Engineering and Architecture, Northwestern Polytechnical University, Xi'an 710072, China
2.MIIT Key Laboratory of Dynamics and Control of Complex Systems, Xi'an 710072, China

ARTICLE INFO

Article history
Received: 28 February 2019
Accepted: 13 March 2019
Published Online: 30 March 2019

Keywords:
Dielectric elastomer balloon
Passive layer
Dynamic behaviour
Active control

ABSTRACT

Dielectric elastomer (DE) balloons are intensively developed as sensors, actuators, and generators. To ensure electrical safety, a DE balloon can be covered by an external passive layer. In this paper, the dynamic behaviours and active control for the DE balloon coupled with the passive layer are investigated. Based on the Hamilton's principle, the dynamic model of the DE balloon covered by the passive layer is derived. With this coupled model, we demonstrate that three typical dynamic responses can appear and the transition among these dynamic behaviours can be achieved by altering the properties of the passive layer. The introduction of the passive layer is able to induce undesirable dynamic behaviours, which require to be controlled. Thus, we present two methods of control including proportional-derivative (PD) control and iterative learning control (ILC). We demonstrate that the undesirable dynamic responses can be effectively eliminated by the proposed methods of control. Particularly, control errors can be reduced by 2 or 3 orders of magnitude using the latter control method. We hope that the present analysis can improve the understanding of dynamic behaviours of a DE balloon covered by a passive layer and promote the control of undesirable dynamic responses.

1. Introduction

Dielectric elastomers (DEs) belong to a category of electro-active polymer, which have been widely used for broad range of applications, such as artificial muscle [1,2], tactile devices [3,4], energy harvesters [5,6], micro-pumps [7,8] and soft robotics [9,10]. Desirable properties include large voltage-triggered deformation, low noise during operation, light weight, low cost, fast response and high energy density [11]. In these DE-based devices, a DE is commonly sandwiched between two flexible electrodes. When a voltage is applied through the electrodes, the opposing charges on each electrode cause the DE to shrink in thickness and expand in area.

An important issue when employing DE-based devices is to ensure electrical safety due to its high operating voltage (generally higher than 1kV) [12]. Coating passive layers on the surfaces of the DEs is an effective method to guarantee electrical safety [13], nevertheless, the introduction of the passive layers certainly affects the voltage-actuated properties, such problem has been discussed in previous research [14,15]. There are versatile shapes for the DEs, such as films, cones, cylinders, rings and balloons. The shape of the DE balloon can be developed for many interesting

**Corresponding Author:*
Zichen Deng,
School of Mechanics, Civil Engineering and Architecture, Northwestern Polytechnical University, Xi'an 710072, China;
E-mail: dweifan@nwpu.edu.cn

DOI: https://doi.org/10.30564/jmer.v2i1.914

applications, including DE pumps, DE balloon generators and soft-handling systems [16]. Bortot considered a DE balloon coated by inner and outer spherical protective passive layers and studied the influence of the passive layers on the static electromechanical responses of the DE balloon [14]. An et al. presented that the passive layer can suppress and eliminate the static electromechanical instability for the DE balloon, and in this way, large voltage-induced deformations can be obtained [15]. However, the existing studies only dealt with the static electromechanical behaviours of the DE balloon coated by the passive layers, and there has been little literature into modelling and analysis of the dynamic characteristics.

Since the DEs have been widely used in various engineering fields, the precise control over the complex dynamic responses of the DEs is important. Research on active control for a single DE have been implemented previously. Wilson et al. presented a bioinspired control scheme, based on cerebellar calibration of the vestibulo-ocular reflex, for adaptive control of nonlinear DE-based artificial muscle [17]. Li et al. implemented the nonlinear visco-hyperelastic DE membranes into a closed-loop control system with PID controller to compensate the undesired dynamic responses of the DE membranes induced by the nonlinear and viscoelastic effects [18]. When coupled with the passive layer, the undesirable dynamic responses for the DE balloons can be triggered, which is not useful for the application and is likely to lead to material failure due to the appearance of the large dynamic deformation. Thus, it is necessary to actively control the dynamic responses of the DE balloon coated by the passive layer.

Motivated by the earlier considerations, this article investigates the dynamic behaviours and active control for a DE balloon coupled with a spherical passive layer. Using the Hamilton's principle, the coupled dynamic model is derived. Based on the proposed dynamic model, we show three typical dynamic responses for the DE balloon by varying the properties of the passive layer. To compensate the undesirable dynamic behaviours of the DE balloon induced by the passive layer, we present two methods including proportional-derivative (PD) control and iterative learning control (ILC) to actively control the DE balloon and passive layer, making the DE balloon applicable to fields where both electrical safety and desirable dynamic behaviours are important.

The rest of this paper is organized as follows. In the second section, we derive a dynamic model for a DE balloon covered by a passive layer. In the third section, three typical dynamic behaviours for the DE balloon coupled with the passive layer are observed. In the fourth section, we introduce two methods of control to eliminate the undesired responses of the DE balloon and obtain precise periodic trajectory tracking. Finally, some conclusions and discussions are drawn.

2. Governing Equations

Figure 1(a) shows a spherical DE balloon of radius R_1 false and thickness H_1 false, which covered by an external passive spherical layer of inner radius R_1 false and outer radius R_2 false. Both sides of the DE balloon are coated with flexible electrodes. The DE balloon is assumed to be thin-walled since a thick DE balloon would require extremely high voltages. For the DE balloon and passive layer, homogeneous deformation along the thickness is assumed. Furthermore, we hypothesize that no relative sliding occurs at the interface between the DE balloon and the passive layer.

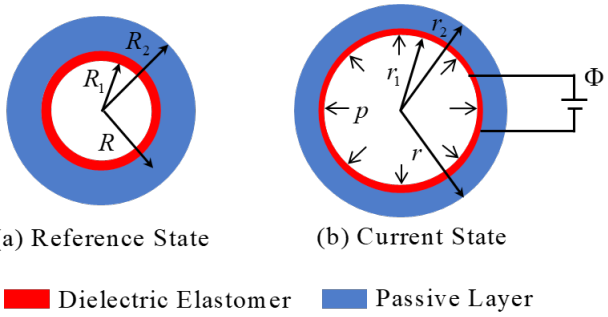

Figure 1. Section of the DE balloon interacting with the passive layer in the reference configuration (a) and a current configuration (b).

As shown in Figure 1(b), in the presence of a constant pressure p inside the DE balloon and a voltage Φ, the DE balloon deforms to radius r_1 and thickness h_1, and the passive layer deforms to inner radius r_1 and outer radius r_2 and the two electrodes gain charges $+Q$ and $-Q$. We consider a material particle as the radius is R in the reference state, and in the current state, the radius becomes r. The corresponding hoop stretch is defined as follows:

$$\lambda(t) = \frac{r(t)}{R}. \tag{1}$$

Then, the coupled system can be described by $(\lambda_1(t), \lambda_2(t))$, where $\lambda_1(t) = r_1(t)/R_1$ and $\lambda_2(t) = r_2(t)/R_2$. We assume that both the DE balloon and the passive layer are incompressible, thus $4\pi R_1^2 H_1 = 4\pi r_1^2 h_1$ for the DE balloon, and for the whole coupled system, the material incompressibility indicates

$$r(t)^3 - r_1(t)^3 = R^3 - R_1^3. \tag{2}$$

 DOI: https://doi.org/10.30564/jmer.v2i1.914

To obtain the velocity field of the coupled system, we need to take the time derivative on both sides of Eq. (2) giving

$$\dot{r} = \frac{r_1^2}{r^2}\dot{r}_1, \tag{3}$$

where $\dot{r}_1 = R_1\dot{\lambda}_1$ and the dot denotes the derivative with respect to t.

2.1. Dynamic Model by the Hamilton's Principle

To derive the dynamic model of the coupled system, the Hamilton's principle is adopted, which takes the form

$$\int_{t_1}^{t_2}(\delta K - \delta\Psi + \delta W_s)dt = 0, \tag{4}$$

where K is the total kinetic energy, Ψ is the total free energy, W_s is the total work of the external stimulus.

2.1.1. Kinetic Energy

The kinetic energy of the coupled system can be expressed as

$$K = \frac{1}{2}\rho_1 4\pi R_1^2 H_1 \dot{r}_1^2 + \frac{1}{2}\int_{r_1}^{r_2}\rho_2 4\pi r^2\dot{r}^2 dr, \tag{5}$$

where ρ_1 and ρ_2 denote the densities of the DE balloon and the passive layer, respectively. The first part in Eq. (5) is the simplified kinetic energy of the DE balloon due to its thin wall.

2.1.2. Free Energy

The model of an ideal DE is adopted to describe the electromechanical behaviour of the DE balloon, which indicates the dielectric behaviour can be unaffected by deformation and the electric displacement D is linear in the electric field E: $D = \varepsilon E$, where ε is the permittivity of the DE balloon taken to be independent of deformation [19]. Here, to account for the strain stiffening effect of the DEs induced by the limited stretch of the polymer chains, we use the Gent model for the DE balloon. Thus, the free energy density of the DE balloon can be written as

$$\psi_1(\lambda_1, D) = -\frac{\mu_1 J_{\lim}}{2}\ln\left(1 - \frac{2\lambda_1^2 + \lambda_1^{-4} - 3}{J_{\lim}}\right) + \frac{D^2}{2\varepsilon}, \tag{6}$$

where μ_1 is the shear modulus of the DE balloon, $J_{\lim}$ is a material constant related to the limiting stretch. Then, we adopt the neo-Hookean model for the passive elastomer layer, and the corresponding free energy density can be written as

$$\psi_2(\lambda) = \frac{\mu_2}{2}(2\lambda^2 + \lambda^{-4} - 3), \tag{7}$$

where μ_2 is the shear modulus of the passive layer.

The total free energy of the DE balloon and the passive layer can be obtained by the integral of the free energy density over the whole volume of the coupled system along the radial direction, as follows:

$$\begin{aligned}\Psi &= \int_{v_1}\psi_1(\lambda_1)dv_1 + \int_{v_2}\psi_2(\lambda)dv_2 \\ &= 4\pi R_1^2 H_1\left[-\frac{\mu_1 J_{\lim}}{2}\ln\left(1 - \frac{2\lambda_1^2 + \lambda_1^{-4} - 3}{J_{\lim}}\right) + \frac{\varepsilon\Phi^2\lambda_1^4}{2H_1^2}\right] + \int_{v_2}\frac{\mu_2}{2}(2\lambda^2 + \lambda^{-4} - 3)dv_2,\end{aligned} \tag{8}$$

where v_1 and v_2 denote the volume of the DE balloon and the passive layer, respectively.

2.1.3. Voltage and Pressure Work

The work done by the external stimulus, including voltage and pressure, can be expressed as $W_s = W_v + W_p$, where W_v and W_p are work terms related to voltage and pressure, respectively. The work done by the voltage can be written as

$$W_v = \Phi Q = C\Phi^2 = 4\pi R_1^2\frac{\varepsilon\Phi^2\lambda_1^4}{H_1}, \tag{9}$$

where Q is the charge on the compliant electrodes, $C = 4\pi\varepsilon r_1^2 / h_1$ is the current capacitance of the DE balloon.

Then, the work done by the pressure can be expressed as

$$W_p = 4\pi p\int_{R_1}^{r_1} r^2 dr - 4\pi p_a\int_{R_2}^{r_2} r^2 dr = \frac{4\pi}{3}p(r_1^3 - R_1^3) - \frac{4\pi}{3}p_a(r_2^3 - R_2^3), \tag{10}$$

where p and p_a are the inner pressure and atmosphere, respectively.

2.2 Equation of Motion

Substituting Eqs. (5), (8), (9) and (10) into Eq. (4) and taking the variations with respect to r_1, we can obtain the equations of motion for the DE balloon covered by the passive layer, which can be written as

$$\begin{cases}\dfrac{d^2\lambda_1}{dT^2} + q(\lambda_1, \lambda_2)\left(\dfrac{d\lambda_1}{dT}\right)^2 + r(\lambda_1, \lambda_2, p, \Phi) = 0, \\ (\lambda_1^3 - 1)R_1^3 = (\lambda_2^3 - 1)R_2^3,\end{cases} \tag{11}$$

where

$$q(\lambda_1, \lambda_2) = \left(\frac{R_1^4}{2R_2^4}\frac{\lambda_1^4}{\lambda_2^4} - \frac{2R_1}{R_2}\frac{\lambda_1}{\lambda_2} + \frac{3}{2}\right)\Bigg/\left[\frac{\rho_1}{\rho_2}\frac{H_1}{R_1}\frac{1}{\lambda_1^2} + \left(\lambda_1 - \frac{R_1}{R_2}\frac{\lambda_1^2}{\lambda_2}\right)\right],$$

$$r(\lambda_1, \lambda_2, p, \Phi) = g(\lambda_1, \lambda_2, p, \Phi)\Bigg/\left[1 + \frac{\rho_2}{\rho_1}\frac{R_1}{H_1}\left(\lambda_1 - \frac{R_1}{R_2}\frac{\lambda_1^2}{\lambda_2}\right)\lambda_1^2\right],$$

DOI: https://doi.org/10.30564/jmer.v2i1.914

$$g(\lambda_1,\lambda_2,p,\Phi)=\frac{2(\lambda_1-\lambda_1^{-5})}{1-(2\lambda_1^2+\lambda_1^{-4}-3)/J_{\lim}}-\frac{(p-p_a)R_1}{\mu_1 H_1}\lambda_1^2-2\frac{\varepsilon\Phi^2}{\mu_1 H_1^2}\lambda_1^3$$
$$+\frac{\mu_2}{\mu_1}\frac{R_1}{H_1}\frac{\lambda_1(\lambda_1-\lambda_2)}{2\lambda_2}\left[4+\left(\frac{1}{\lambda_1}+\frac{1}{\lambda_2}\right)\left(\frac{1}{\lambda_1^2}+\frac{1}{\lambda_2^2}\right)\right],$$

and the second equation in Eq. (11) gives the coupling deformation relationship between the DE balloon and the passive layer, which is obtained by inserting $r=r_2$ and $R=R_2$ into Eq. (2). Besides, $T=t/R_1\sqrt{\rho_1/\mu_1}$, $(p-p_a)R_1/\mu_1 H_1$ and $\Phi\sqrt{\varepsilon/\mu_1}/H_1$ denote the dimensionless time, the dimensionless pressure and the dimensionless voltage, respectively.

For convenience of analysis, the following dimensionless parameters are defined as

$$M=\frac{\mu_2}{\mu_1},G=\frac{R_2}{R_1},$$

where M and G are the shear modulus ratio and the geometry ratio between the passive layer and the DE balloon, respectively.

In the following numerical calculation, a commercially available acrylic elastomer VHB4910 (3M Company) is employed for the DE balloon with the following material parameters: $\varepsilon=3.98\times10^{-11}$ F/m, $\mu_1=65$ KPa, and $J_{\lim}=120$. Without loss of generality, the radius and the thickness of the DE balloon are fixed as R_1 = 10 mm and H_1 = 1 mm, respectively.

3. Dynamic Response under Parametric Excitation

In this section, we investigate the effect of the passive layer on the dynamic responses of the DE balloon. Specifically, by varying the value of G or M, we present three typical nonlinear dynamic behaviour for the DE balloon induced by the introduction of the passive layer.

Consider that the DE balloon is subject to a sinusoidal voltage:

$$\Phi(t)=\Phi_{dc}+\Phi_{ac}\sin(\Omega t), \tag{12}$$

where Φ_{dc} is the DC voltage, Φ_{ac} and Ω are the amplitude and excitation frequency of the AC voltage, respectively. Substituting Eq. (12) into Eq. (11) yields

$$\begin{cases}\dfrac{d^2\lambda_1}{dT^2}+q(\lambda_1,\lambda_2)\left(\dfrac{d\lambda_1}{dT}\right)^2+r(\lambda_1,\lambda_2,p,\tilde{\Phi}_{dc},\tilde{\Phi}_{ac},\tilde{\Omega})=0,\\ (\lambda_1^3-1)R_1^3=(\lambda_2^3-1)R_2^3,\end{cases} \tag{13}$$

where $\tilde{\Phi}_{dc}=\Phi_{dc}\sqrt{\varepsilon/\mu_1}/H_1$ is the dimensionless DC voltage, $\tilde{\Phi}_{ac}=\Phi_{ac}\sqrt{\varepsilon/\mu_1}/H_1$ is the dimensionless AC voltage and $\tilde{\Omega}=\Omega R_1\sqrt{\rho_1/\mu_1}$ is the dimensionless excitation frequency. In the following analysis, the Runge-Kutta integrator is employed to calculate the dynamic response of the DE balloon covered by the passive layer. We assume that the DE balloon deforms with the initial conditions: $\lambda_1(0)=\lambda_{eq},\dot{\lambda}_1(0)=0$, i.e., the balloon is initially at rest, where λ_{eq} is the stable equilibrium stretch of the DE balloon under the constant DC voltage only.

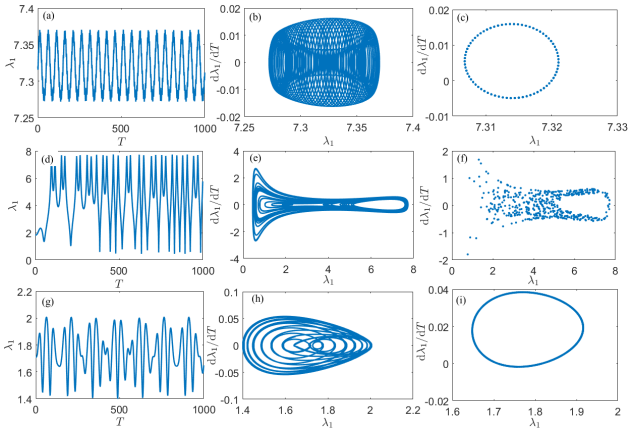

Figure 2: Under a parametric combination of DC and AC voltages

Note: Three typical nonlinear dynamic responses (a), (d), (g); phase paths (b), (e), (h); and Poincare maps (c), (f), (i) of the DE balloon covered by the passive layer. Three different values of G are used in the simulation: G = 3 for (a), (b), (c); G = 5 for (d), (e), (f); G = 8 for (g), (h), (i).

Without loss of generality, we study the influence of the passive layer on the dynamic behaviour of the DE balloon by varying the value of G. Here, the value of M is set as $M=0.11$, the value of static pressure is set as $(p-p_a)R_1/\mu_1 H_1=2.5$, the parameters of applied voltage are fixed as $\tilde{\Phi}_{dc}=0.1$, $\tilde{\Phi}_{ac}=0.05$ and $\tilde{\Omega}=2\pi/50$. When we change the value of G, three typical oscillation can be observed as shown in Figure 2, where the dynamic responses, phase paths and Poincare maps of the DE balloons coupled with different properties of the passive layer are plotted. The phase paths and Poincare maps can be utilized to further explore the dynamic characteristics of the coupled system [20,21]. If only one point appears in Poincare maps, the coupled system undergoes a periodic oscillation. If a closed loop in Poincare maps is formed by discrete points, the coupled system experiences quasi-periodic oscillation. Conversely, if the points in the Poincare maps are disordered, the coupled system undergoes aperiodic oscillation.

When $G=3$, the DE balloon experiences a nonlinear oscillation, and the closed Poincare map indicates that the dynamic response is quasi-periodic steady oscillation, as sketched in Figures 2(a)-(c). When $G=5$, it can be found that the dynamic snap-through behaviour occurs [22,23], i.e., the DE balloon could jump dramatically be-

DOI: https://doi.org/10.30564/jmer.v2i1.914

tween a slightly stretched state and a largely stretched state (Figure 2(d)). Moreover, the points in Poincare maps are disordered shown in Figure 2(f), representing that varying the properties of the passive layer leads to an aperiodic oscillation for the DE balloon. Another interesting phenomenon is that the deformation of the DE balloon is upper bounded (Figure 2(d)), which results from the strain-stiffening effect of the DEs. When $G=8$, from Figure 2(i), it can be seen that the Poincare map forms a closed loop indicating that a quasi-periodic oscillation occurs. However, as depicted in Figure 2(g), the dynamic response under this case is beat oscillation, i.e., the DE balloon experiences a fast oscillation but with slowly variable sinusoidal amplitude. The appearance of the beating phenomenon is caused by two sinusoidal factors of different angular frequencies in dynamic response of DE balloon, where the oscillation frequency and the amplitude are determined by the more rapid one and the slower one, respectively. Therefore, it can be observed that, when the properties of the passive layer change, the dynamic responses of the DE balloon experience the transition between quasi-periodic oscillation and aperiodic oscillation, especially, beating oscillation can appear at certain conditions.

The dynamic behaviour of the DE balloon is dependent on the passive layer. Under the same sinusoidal voltage excitation, different conditions of the passive layer can result in disparate nonlinear dynamic responses, which is not undesirable for the practical applications. In the following section, we will demonstrate that, by using the active control, the response uncertainties of the DE balloon due to the coupling with the passive layer can be eliminated and the desired responses can be obtained.

4. Active Control

Precise trajectory output is essentially important for a DE balloon covered a passive layer. However, some undesired dynamic behaviours of the DE balloon are encountered under the influence of the passive layer. In this section, the active control methods are proposed to eliminate the undesired response of the DE balloon and obtain precise periodic trajectory tracking. Since the dynamic model of the DE balloon is highly nonlinear, model-free control algorithms are considered. More specifically, proportional-derivative (PD) control and iterative learning control (ILC)methods are adopted.

4.1 Proportional-derivative control

Proportional-integral-derivative (PID) control is the most widely used control method, and it has numerous applications in engineering such as robots, spacecraft, and structures [18, 24-26]. The control action is calculated based on the error as well as the derivative and the integral of the error between the desired output and the measured output. The integral part of the PID controller contributes to eliminate the steady-state error in the case that the desired output is a constant. However, in the case of periodic trajectory tracking, some researchers prefer not to use the integral part, reducing to the proportional-derivative (PD) control. Therefore, the PD control method is adopted to eliminate the undesired dynamic response of the DE balloon and track the desired trajectory.

The desired response of the DE balloon is considered as a sinusoidal oscillation around λ_{eq}, written as

$$\lambda_{1\mathrm{d}} = \lambda_{eq} + A\sin\left(\tilde{\Omega}T\right) \tag{14}$$

where the amplitude $A=0.05$ is adopted in the simulations. The input voltage Φ_{In} of the system is calculated by

$$\Phi_{\mathrm{In}} = \max\left(0, \Phi_{\mathrm{E}} + \Phi_{\mathrm{PD}}\right), \tag{15}$$

where Φ_{E} is the excitation voltage and Φ_{PD} is the feedback control voltage calculated by PD control method. Note that, Φ_{In}, Φ_{E} and Φ_{PD} denote dimensionless voltages in following analysis. It is worth noting that when the voltage becomes negative, it also stretches the DE balloon as if it is positive. However, in the control theory when the input becomes negative, the input is supposed to have an opposite effect on the system. Since the negative voltage cannot produce an opposite effect on the DE balloon, the input voltage is limited to positive by a maximum function in Eq. (15). The feedback control voltage is calculated by

$$\Phi_{\mathrm{PD}} = K_{\mathrm{P}}e + K_{\mathrm{D}}\dot{e} \tag{16}$$

where K_P and K_D are proportional and derivative gains respectively, $e=\lambda_{1d}-\lambda_1$ is the error between the desired output and the actual output (it is assumed that it can be measured accurately without time delay). The gains K_P and K_D are determined manually based on the influence of the gains on the control results [18]. The effects of the PD controller on the dynamic behaviours of the DE balloon coveredby the passive layer will be shown in the following simulations.

Table 1. Proportional and derivative gains in the simulations

G	3	5	7
K_{P}	5	2	3
K_{D}	5	8	15

DOI: https://doi.org/10.30564/jmer.v2i1.914

The simulations focus on the typical dynamic behaviours as shown in the last section, which are quasi-periodic oscillation, aperiodic oscillation, and beating oscillation for $G=3$, $G=5$, and $G=7$ respectively. The values of the proportional and derivative gains in the simulations are shown in Table 1. It can be seen from Figure 3(a) that the response of the PD controlled DE balloon appears to be sinusoidal despite of the values of G. By comparing with the dynamic behaviours without PD control in Figure 2, it is found that the PD controller effectively eliminate the quasi-periodic oscillation, aperiodic oscillation, and beating oscillation of the DE balloon coveredbythe passive layer. The control errors of the DE balloon are shown in Figs 3(b). It can be found that the control errors are also periodic. The maximum control errors are about 5.7 %, 45.5 %, and 21.9 % of the desired oscillation amplitude for $G=3$, $G=5$, and $G=7$ respectively, which are too large for the DE balloon. Although increasing the proportional and derivative gains could reduce control errors, the system would be more sensitive to measurement noise in practice. Therefore, a new controller will be proposed combined with ILC in the next subsection to further improve the control accuracy of the DE balloon without changing the proportional and derivative gains.

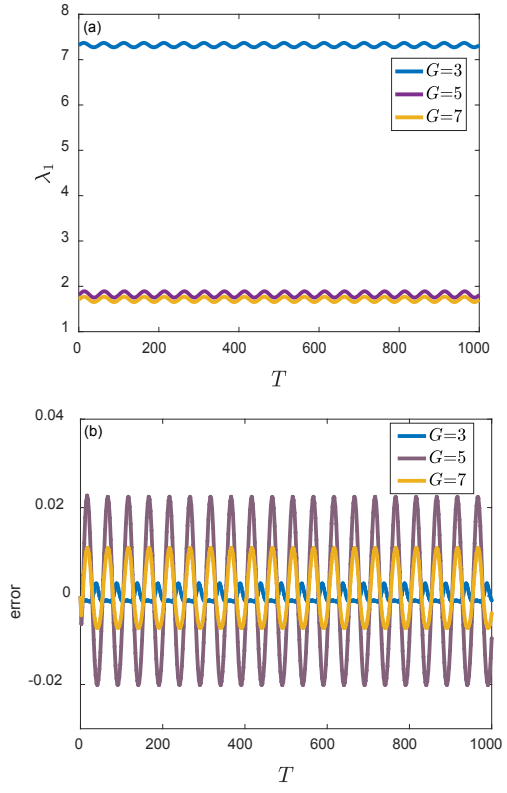

Figure 3. Under the excitation voltages and a PD controller, dynamic responses (a) and the control errors (b) of the DE balloon covered by the passive layer.

4.2 Iterative Learning Control

ILC is a model-free control method for batch operations that improves the control accuracies of the current operation by using the control inputs and outputs of the previous operations.In order to improve the control accuracy in the periodic trajectory tracking problem of the DE balloon, the ILC method is combined with the PD control method.

The control voltage of the current period is obtained based the control voltage of the last period. The input voltage in the kth period of this new ILC-PD controller is calculated by

$$\Phi^k = \max\left(0, \Phi_{\mathrm{E}}^k + \Phi_{\mathrm{PD}}^k + \Phi_{\mathrm{ILC}}^k\right) \tag{17}$$

where Φ_{PD}^k is obtained by Eq. (16), and Φ_{ILC}^k is the feedforward control voltage obtained by ILC method. In order to design Φ_{ILC}^k, two basic principles should be noticed. Firstly, from the simulation results of Figure 3, the first period is devoted to reducing initial error and obtaining periodic oscillation. Therefore, the learning process should begin at the third period using the information of the second period. Thus Φ_{ILC}^k should be 0 for the first and second periods. Secondly, the PD control scheme should be smoothly switched to ILC-PD scheme at the beginning of the third period, so that the sudden change of the input voltage, as well as the dynamic behaviours of the DE balloon, can be avoided. Based on the above two principles and the ILC controller in literature [27], $\Phi_{\mathrm{ILC}}^{k+1}$ can be designed as

$$\Phi_{\mathrm{ILC}}^{k+1} = K_{\mathrm{ILC}}\left(\Phi_{\mathrm{ILC}}^k + \Phi_{\mathrm{PD}}^k\right) \tag{18}$$

where

$$K_{\mathrm{ILC}} = \begin{cases} 0, & T<100, \\ \tanh\left(\dfrac{T-100}{50}\right), & T \geq 100. \end{cases} \tag{19}$$

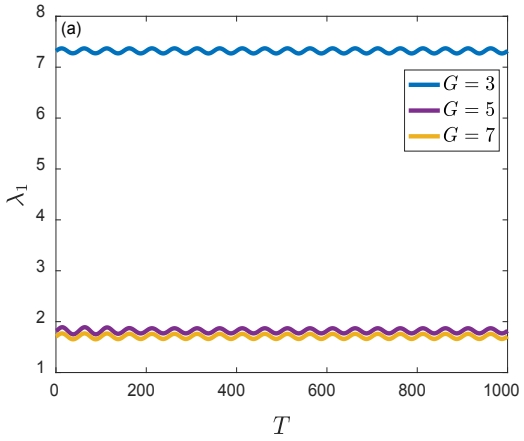

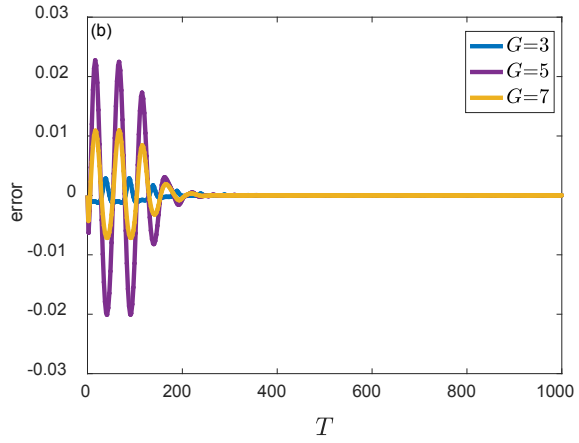

Figure 4. Under the excitation voltages and an ILC-PD controller, dynamic responses (a) and the control errors (b) of the DE balloon covered by the passive layer.

The simulations are carried out to validate the effectiveness of the ILC-PD controller for $G=3$, $G=5$, and $G=7$. The gains are shown in Table 1, and the simulation results are depicted in Figure 4. Before the ILC scheme is switched on ($T<100$), the dynamic behaviours of the system are exactly the same as those of the PD controlled system in Figure 3. However, after switching on the ILC scheme, the magnitudes of the dynamic responses change gradually and the frequencies appear unchanged, as seen in Figure 4(a). Figure 4(b) illustrates that the control errors of the DE balloon actuator are reduced greatly for $T \geq 100$. The maximum errors, after they reach the steady periodic oscillation, become 0.015%, 0.068%, and 0.026% of the desired oscillation amplitude for $G=3$, $G=5$, and $G=7$ respectively.

It can be concluded from the above analyses that the ILC method contributes to reduce the trajectory tracking errors of the PD control method by 2-3 orders of magnitude. Therefore, the proposed ILC-PD controller is suitable for high-precision periodic trajectory tracking of the DE balloon covered by different properties of the passive layers.

4.3 Accuracies and Stabilities of the Controllers

In the above simulations, the PD controller and the ILC-PD controller have been demonstrated to eliminate the undesired dynamic behaviours and improve trajectory tracking accuracies. However, the effects of the proportional and derivative gains on the controlled system are not addressed. Due to the complexity and nonlinearity of the system and environment, it is not easy to study the stabilities of the controller theoretically. Therefore, the authors would like to study the effects of the proportional and derivative gains on the accuracies and stabilities of the controllers numerically in this subsection.

Although the control errors are dependent on G, the tendencies of the control errors with respect to the control gains are similar for different value of G. Thus, $G=5$ is considered in this subsection. In the simulations, both K_P and K_D vary from 0 to 20 with the increment of 1, and all the combinations of K_P and K_D are studied. The simulation results are presented in Figure 5. The maximum errors are estimated in the steady state, i.e. the 10th-20th periods for the PD controller and 15th-20th periods for the ILC controller.

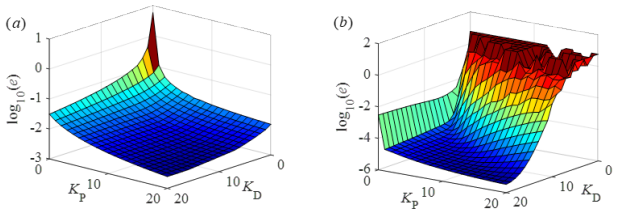

Figure 5. Effects of proportional and derivative gains on the maximum control errors of the controllers for $G=5$: PD controller for (a), and ILC-PD controller for (b).

Before studying the stability of the controllers, a stability criterion should be introduced. Since the desired oscillation amplitude is 0.05, the controller can be roughly considered stable if the maximum control error is smaller than 0.05. Under this criterion, it can be clearly seen from Figure 5that the stable region of the PD controller is much larger than the ILC-PD controller, although the accuracies of the ILC-PD controller are much high in the stable region. The accuracy of the PD controller increases as K_P or K_D increases. And the effect of K_P on the accuracy of the PD controller is larger than that of K_D. However, K_D has a dominant effect on the stability and accuracy of the ILC-PD controller. The ILC-PD controller becomes unstable if K_D is too small. As K_P increases, a larger K_D should also be chosen to guarantee the stability of the controlled system. In summary, a small K_P and a moderate K_D should be chosen for the ILC-PD controller.

5. Conclusions

This paper investigates dynamic behaviours and active control of a DE balloon covered by an external passive layer. Using the Hamilton's principle, the motion of equation for the DE balloon coupled with the passive layer is derived. Based on the coupled model, we observe three typical dynamic responses including quasi-periodic oscillation, aperiodic oscillation and beating oscillation. Furthermore, the transition among these types of dynamic responses can be realized by varying the properties of the passive layer. The undesired dynamic behaviours of the

DOI: https://doi.org/10.30564/jmer.v2i1.914

DE balloon due to the introduction of the passive layer require to be eliminated, which can be achieved by a simple PD controller, however with large control errors. In order to further improve control accuracy, the ILC method is introduced, and an ILC-PD controller is proposed. Simulation results show that the control errors can be reduced by 2 or 3 orders of magnitude using the proposed ILC-PD controller. We hope that the present analysis can improve the understanding of dynamic behaviours of a DE balloon covered by a passive layer and promote the control of undesirable dynamic responses.

Acknowledgments

This work is supported by the National Natural Science Foundation of China (91648101, 11432010), and also is supported by Innovation Foundation for Doctor Dissertation of Northwestern Polytechnical University (CX201910).

References

[1] Anderson I A, Gisby T A, Mckay T G, et al. Multi-functional dielectric elastomer artificial muscles for soft and smart machines, Journal of Applied Physics, 2012, 112: 041101.

[2] Carpi F, Kornbluh R, Sommer-Larsen P, et al. Electroactive polymer actuators as artificial muscles: are they ready for bioinspired applications? Bioinspiration & Biomimetics, 2011, 6:045006.

[3] Lee H S, Phung H, Lee D H, et al. Design analysis and fabrication of arrayed tactile display based on dielectric elastomer actuator. Sensors and Actuators A: Physical, 2014, 205:191-198.

[4] Shikida M, Imamura T, Ukai S, et al. Fabrication of a bubble-driven arrayed actuator for a tactile display. Journal of Micromechanics and Microengineering, 2008, 18(6):065012.

[5] Henann D L, Chester S A, Bertoldi K. Modeling of dielectric elastomers: Design of actuators and energy harvesting devices[J]. Journal of the Mechanics and Physics of Solids, 2013, 61(10):2047-2066.

[6] Chiba S, Waki M, Wada T, et al. Consistent ocean wave energy harvesting using electroactive polymer (dielectric elastomer) artificial muscle generators. Applied Energy, 2013, 104:497-502.

[7] Li Z, Wang Y, Foo C C, et al. The mechanism for large-volume fluid pumping via reversible snap-through of dielectric elastomer. Journal of Applied Physics, 2017, 122(8):084503.

[8] Tavakol B, Bozlar M, Punckt C, et al. Buckling of dielectric elastomeric plates for soft, electrically active microfluidic pumps. Soft Matter, 2014, 10(27):4789-4794.

[9] Shian S, Bertoldi K, Clarke D R. Dielectric Elastomer Based "Grippers" for Soft Robotics. Advanced Materials, 2015, 27(43):6814-6819.

[10] Xu L, Chen H Q , Zou J, et al. Bio-inspired annelid robot: a dielectric elastomer actuated soft robot. Bioinspiration & Biomimetics, 2017, 12(2):025003.

[11] Suo Z. THEORY OF DIELECTRIC ELASTOMERS. Acta Mechanica Solida Sinica, 2010, 23(6):549-578.

[12] Pourazadi S, Shagerdmootaab A, Chan H, et al. On the Electrical Safety of Dielectric Elastomer Actuators in Proximity to the Human Body. Smart Materials and Structures, 2017, 26:115007.

[13] Luigi C, Gabriele F, Massimiliano G , et al. Active compression bandage made of electroactive elastomers. IEEE/ASME Transactions on Mechatronics, 2018, 23:2328-2337.

[14] Bortot, Eliana. Analysis of multilayer electro-active spherical balloons. Journal of the Mechanics and Physics of Solids, 2017, 101:250-267.

[15] An S Q, Zou H L and Deng Z C. Control instability and enhance performance of a dielectric elastomer balloon with a passive layer. Journal of Physics D: Applied Physics, 2019, 52:195301.

[16] Wang T, Zhang J, Hong , et al. Dielectric Elastomer Actuators for Soft Wave-Handling Systems. Soft Robotics, 2017, 4(1):61-69.

[17] Wilson E D, Assaf T, Pearson M J, et al. Cerebellar-inspired algorithm for adaptive control of nonlinear dielectric elastomer-based artificial muscle. Journal of The Royal Society Interface, 2016, 13(122):20160547.

[18]Y. Li, I. Oh, J. Chen, et al. Nonlinear dynamic analysis and active control of visco-hyperelastic dielectric elastomer membrane, International Journal of Solids and Structures, 2018, 152-153:28-38.

[19] Zhao X, Hong W, Suo Z . Electromechanical hysteresis and coexistent states in dielectric elastomers. Physical Review B, 2007, 76(13):134113.

[20] Zhang J, Chen H, Li D. Method to Control Dynamic Snap-Through Instability of Dielectric Elastomers. Physical Review Applied, 2016, 6(6):064012.

[21] Sheng J, Chen H, Liu L, et al. Dynamic electromechanical performance of viscoelastic dielectric elastomers. Journal of Applied Physics, 2013, 114(13):134101.

[22] Chen F, Zhu J, Wang M Y. Dynamic electromechanical instability of a dielectric elastomer balloon. Epl, 2015, 112(4):47003.

[23] Li B, Zhang J, Chen H, et al. Voltage-induced pinnacle response in the dynamics of dielectric elastomers. Physical Review E, 2016, 93(5):052506.

 DOI: https://doi.org/10.30564/jmer.v2i1.914

[24] Rustemli S , Yilmaz M , Demirtas M . Ripple reduction at speed and torque of step motors used on a two-axis robot arm[J]. Robotics and Computer-Integrated Manufacturing, 2010, 26(6):759-767.

[25] Pounds P E I , Dollar A M . Stability of Helicopters in Compliant Contact Under PD-PID Control[J]. IEEE Transactions on Robotics, 2014, 30(6):1472-1486.

[26] Parra-Vega V , Arimoto S , Liu Y H , et al. Dynamic sliding PID control for tracking of robot manipulators: theory and experiments[J]. IEEE Transactions on Robotics and Automation, 2003, 19(6):967-976.

[27] Q. Li, Z. Deng, K. Zhang, et al. Precise Attitude Control of Multirotary-Joint Solar-Power Satellite, Journal of Guidance, Control, and Dynamics, 2018, 41:1435-1442.

DOI: https://doi.org/10.30564/jmer.v2i1.914